Chemical Compositions and Tectonic Significance of Chrome-Rich Spinels in the Tianba Flysch, Southern Tibet

Bin Zhu, William S. F. Kidd, David B. Rowley,[1] *and Brian S. Currie*[2]

Earth and Atmospheric Sciences, State University of New York, Albany, New York 12222, U.S.A.
(e-mail: bz7463@csc.albany.edu)

ABSTRACT

Turbiditic sandstones from the mid–Late Cretaceous Tianba Flysch sequence are well exposed near Tianba in the north Nieru Valley, southern Tibet, and contain significant amounts of chrome-rich spinels. Microprobe results show that the spinels have a well-developed Fe-Ti trend and have Cr/(Cr + Al) 0.4–0.65, Mg/(Mg + Fe^{2+}) 0.3–0.9, and TiO_2 >1%. The occurrence of melt inclusions, and well above 0.2% TiO_2 contents, shows that a volcanic suite of rocks was the source of these Cr-rich spinels. Specifically, these spinels compositionally resemble spinels from intraplate basalts (e.g., Hawaii and Disko Island, western Greenland) rather than from ophiolitic ultramafic or gabbroic material expected in an intraoceanic subduction system associated with the closing of the Neo-Tethys. On the basis of paleotectonic reconstruction, the presence of mid–Late Cretaceous fossils in the strata, and the limited range of chemical compositions, we suggest that 117-Ma volcanics of the Rajmahal-Kerguelen hot spot were the source for the chrome-rich spinels in the Tianba Flysch.

Introduction

The petrologic, mineralogic, and geochemical characteristics of sedimentary basin deposits can greatly aid in reconstructing the tectonic evolution of adjacent orogenic belts (Dickinson and Suczek 1979; Zuffa 1980; Ingersoll et al. 1984; Dickinson 1985; Garzanti et al. 1996; Dewey and Mange 1999). The original composition of sediment source lithologies, however, may be obscured by many factors, including climate, relief, transport mechanism, postburial diagenesis, and regional metamorphism (Morton 1985, 1991). Since chemically and mechanically unstable minerals are altered or eliminated by weathering and diagenesis, studies of resistant minerals in sedimentary rocks are applied in paleotectonic reconstructions with increasing frequency (Morton 1991; Caironi et al. 1996; Lihou and Mange-Rajetzky 1996; Sciunnach and Garzanti 1996; Cookenboo et al. 1997; Dewey and Mange 1999). Of these resistant minerals, chromian spinel is of particular significance to sedimentary provenance studies for a variety of reasons: (1) spinels crystallize from mafic and ultramafic magmas over a wide range of conditions and therefore are a sensitive indicator of the original host magmatic rock composition (Irvine 1967; Allan et al. 1988; Roeder 1994). (2) The unusual chemical durability of chromian spinel makes its original composition more likely to be preserved against processes of weathering and diagenesis. (3) The hardness and lack of cleavage make spinel physically resistant to mechanical breakdown. As such, detrital spinel has the potential to survive weathering and transport processes and exist as a heavy-mineral component of clastic sedimentary rocks (Pober and Faupl 1988; Cookenboo et al. 1997; Ganssloser 1999; Lenaz et al. 2000). (4) Since compositional analysis of spinels is routinely applied in petrologic studies of spinel-bearing igneous rocks, a large volume of microprobe data is available in the literature (Dick and Bullen 1984; Arai and Okada 1991; Arai 1992; Lee 1999; Barnes and Roeder 2001; Kamenetsky et al. 2001).

Recently, there has been a great deal of interest in the early tectonic history of the Himalaya, the orogenic product of continent-continent collision between Asia and India (Tapponnier et al. 1981;

Manuscript received June 10, 2003; accepted January 15, 2004.

[1] Department of Geophysical Sciences, University of Chicago, Chicago, Illinois 60637, U.S.A.

[2] Department of Geology, Miami University, Oxford, Ohio 45056, U.S.A.

[The Journal of Geology, 2004, volume 112, p. 417–434] 0022-1376/2004/11204-0003$15.00

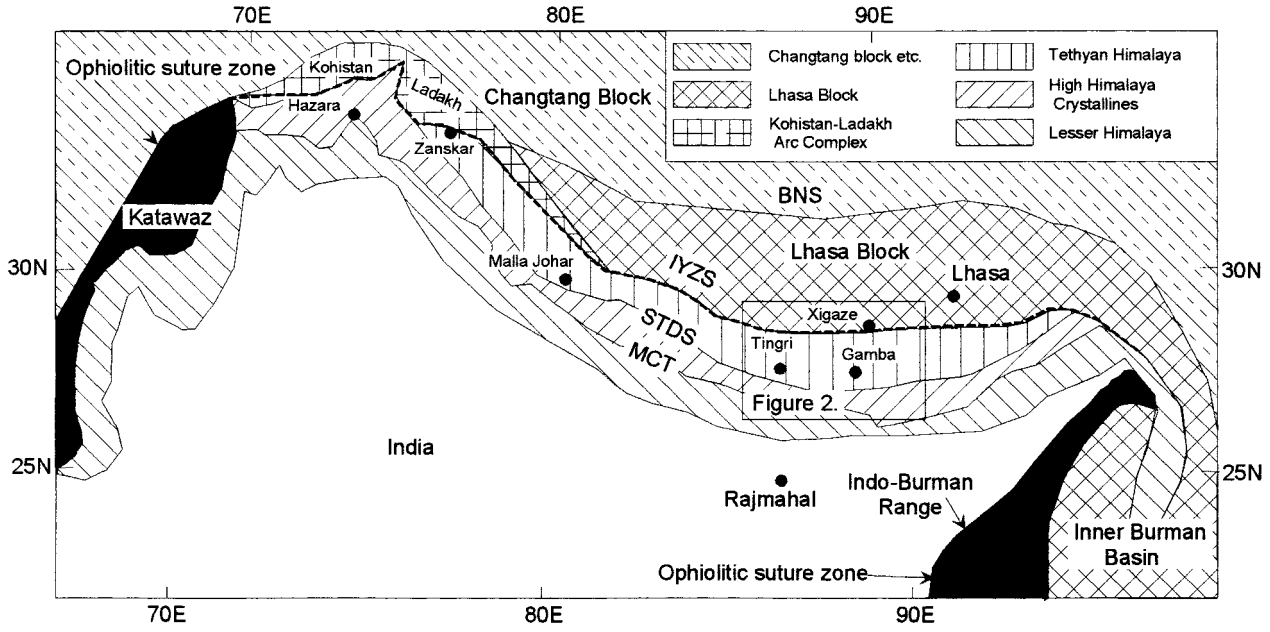

Figure 1. Regional geological map of Tethyan Himalaya (after Rowley 1996). *BNS* = Banggong-Nujiang suture; *IYZS* = Indus-Yarlung-Zangbo suture; *MCT* = Main Central Thrust; *STDS* = Southern Tibet Detachment System.

Allegre et al. 1984; Wang et al. 2000; Yin and Harrison 2000; Wan et al. 2001; Ziabrev et al. 2001; Davis et al. 2002). Much of the pre–middle Tertiary record of this tectonism is recorded in the sedimentary rocks situated south of the Indus-Yarlung-Zangbo suture in southern Tibet (Garzanti et al. 1987, 1996; Garzanti 1993, 1999; Beck et al. 1995; Rowley 1996, 1998). Although the initial collision of India and Asia is believed to have begun during the mid-Tertiary (Garzanti et al. 1987; Rowley 1996, 1998; Wan et al. 2001), less is known about the earlier history of Himalayan orogenesis. In this article, we report provenance data from the Cretaceous Tianba Flysch of the Nieru Valley in the Tethyan Himalaya to better understand the tectonic history of the region. The Tianba Flysch consists of a section of lithic-rich turbidite sandstones and interbedded shales, which in terms of its lithology and bedding characteristics appears in outcrop to be a typical collision-related flysch deposit (Rowley and Kidd 1981; Garzanti et al. 1987) and might be presumed to record an arc-continent collision or ophiolite-obduction event in the mid–Late Cretaceous (Searle 1983). Our data provide insight into the early evolution of Himalayan orogensis and allow a clear test of the hypothesis that there was a mid–Late Cretaceous ophiolite-obduction event in the eastern Tethyan Himalaya during the mid–Late Cretaceous.

Geologic Overview

The Tethyan Himalaya, which lie between the High Himalayan Crystalline belt to the south and the Indus-Zangbo suture and the Lhasa block to the north (fig. 1), consist primarily of Late Paleozoic to Early Eocene sedimentary rocks, originally deposited along the northern edge of the Indian continent. Deposition began with a Late Paleozoic-Triassic rifting (Sengor et al. 1988; Sciunnach and Garzanti 1996; Garzanti 1999) during the initial development of the Neo-Tethyan Ocean. During the Mesozoic, a relatively wide passive continental margin subsequently developed along the north rim of the Indian continent. In mid-Cretaceous time, northward-directed subduction of the Neo-Tethyan oceanic crust beneath the southern margin of Asia resulted in the development of a magmatic arc and a fore-arc-related basin (Xigaze fore-arc basin) along the southern margin of the Lhasa block (Einsele et al. 1994; Durr 1996). With continued subduction, the India-Asia collision initiated in the early Tertiary and produced the Indus-Yarlung-Zangbo suture. Therefore, the strata of the Tethyan Himalaya record the entire depositional history of the northern Indian passive margin.

In southern Tibet, the Tethyan Himalaya can be divided into two subzones of different lithologic assemblages (fig. 2) that are separated by the east-

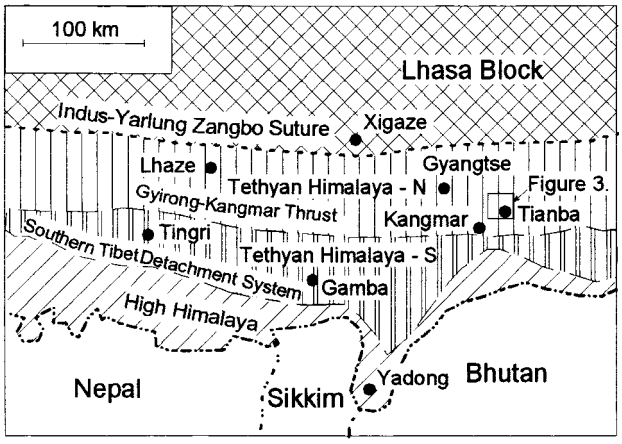

Figure 2. Simplified tectonic map of the study area (after Willems et al. 1996).

west trending Gyirong-Kangmar thrust (Burg and Chen 1984; Liu 1992). The northern zone is dominated by slightly metamorphosed deposits of outer shelf, continental slope, and rise environments, whereas the southern zone is characterized by nonmetamorphic, shallow-water shelf calcareous and terrigenous deposits ranging from Late Paleozoic to Eocene (Wen 1987; Xizang BGMR 1992; Willems et al. 1996).

This study concentrates on the well-exposed lithic-rich arenites at the northern end of the Nieru Valley (fig. 3), which belong to the northern zone of the Tethyan Himalaya. Near Tianba, the lower part of the section consists of thin-bedded gray shales, silty shales, and cherts of the Jiabula Group (Liu 1992; Xizang BGMR 1992). These rocks contain abundant fossils of nektonic organisms including ammonites and belemnites, which indicate a Berriasian-Aptian age (Wang et al. 2000; Z. Binggao, pers. comm., 2000). The Jiabula Group contains pyrite concretions, dark shales, and laminated grayish-green cherts indicating deposition within deep-water, sediment-starved basin (Liu 1992; Wang et al. 2000).

The upper part of the Jiabula Group in the northern Nieru Valley is made up of the Tianba Flysch. In this area, the Tianba Flysch is about 220 m thick (fig. 4) and consists primarily of well-bedded sandstone, siltstones, and shales. The contact between the Tianba Flysch and the underlying dark shales and cherts is conformable. The basal interval of the flysch is characterized by a transition from black cherts to olive-colored argillites and mica-rich siltstones that rapidly coarsen upward into the graded sandstones (fig. 5). Individual sandstone beds fine upward into siltstones and shales and contain abundant sedimentary structures including sole marks, horizontal laminations, and ripple cross-laminations. These rocks are interpreted as Bouma-type turbidites and indicate deep water, continental rise, or perhaps slope environment.

The Tianba Flysch is conformably overlain by greenish-gray burrowed shales that contain a few thin sideritic sandstone beds, and an interval containing some large (up to 1-m diameter) calcareous nodules, one of which yielded an ammonite. Belemnites are also found in the shales above the flysch, and preliminary investigation of radiolarian fossils in the sideritic sandstones points to a Late Cretaceous age of deposition (N. Shafique, pers. comm., 2002).

Above the concretionary shales, a significant fault places mélange, including blocks of pink limestones (Chuangde "formation"; Wang et al. 2000), over the dipping and folded Cretaceous rocks described previously (fig. 4). The pink limestone blocks in the hanging wall of this fault contain abundant foraminifera (*Globotruncana linneiana, G. elevata, Marginotruncana stuarti, M. stuartiformis, Heterohelix* sp) that indicate a Campanian depositional age (Willems et al. 1996; Wang et al.

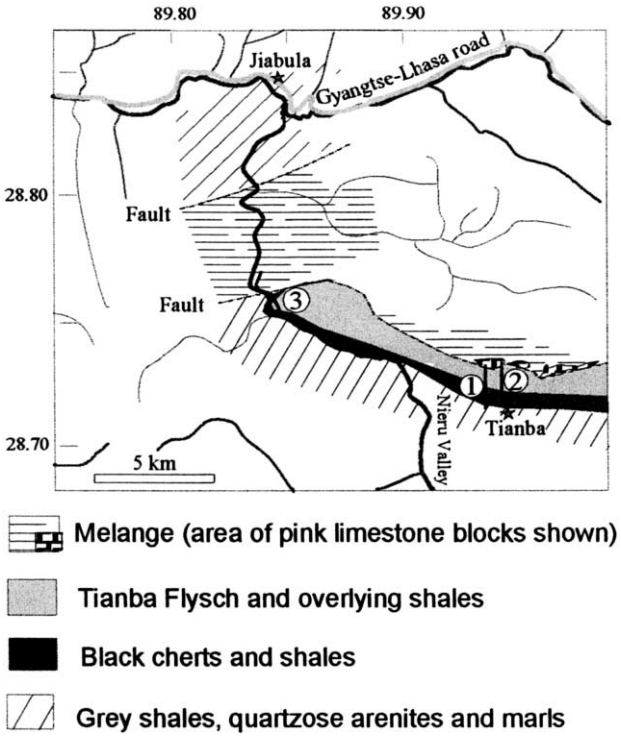

Figure 3. Sketch geologic map of the northern Nieru Valley showing locations of three measured sections.

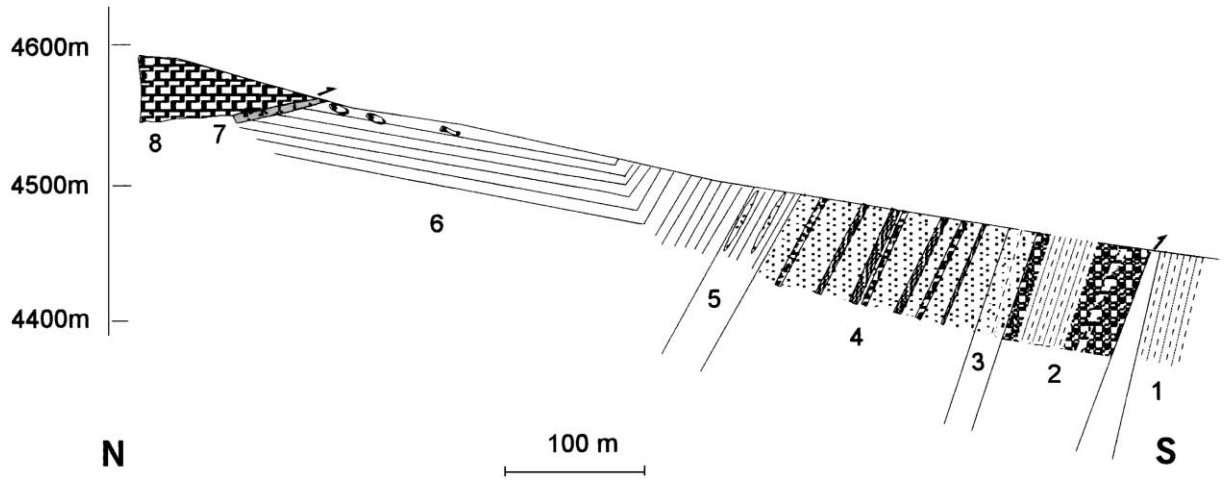

Figure 4. Tianba cross section (section 2; see fig. 3 for location). Unit numbers correspond to those on the stratigraphic column (fig. 5), which includes explanation of the patterns.

2000; N. Shafique, pers. comm., 2002). Based on the sedimentologic, structural, and biostratigraphic data, the Tianba Flysch was deposited during mid-Cretaceous time in a deep-water setting of the outer Indian passive margin.

Detrital Modes of Tianba Flysch

Petrographic examination of the samples from the northern Nieru Valley indicates that there are two types of sandstone associated with the Tianba Flysch. In the lower part of the unit, and mostly in the western sections (fig. 3), the first sandstone beds are primarily quartz-rich lithic arenites. Most of the sandstones above, by contrast, are lithic wackes.

In the basal part of the western section (fig. 6), arenites are greenish in color and occur as strongly channeled lensoidal bodies within the uppermost 25 m of the dark cherts and siliceous shales of the Jiabula Group. Quartz constitutes 52%–81% of the total framework grains. Matrix content is generally less than 15%. Average percentages of monocrystalline and polycrystalline quartz (Qm, Qp) are 70% and 1%, respectively. Lithic fragments, the second-most abundant constituent, comprise 5%–28% of the total framework grain population. These lithic grains can be further divided into volcanic (Lv), metamorphic (Lm), and sedimentary (Ls) types on the basis of relict features. The recalculated mean value of LvLmLs parameters of quartz-rich arenites are 8%, 80%, and 12%, respectively, showing that these sandstones are most likely derived from a metamorphic terrane. Feldspar content is minor, averaging 1% of the total grain population.

The recalculated mean value of QtFL plots (fig. 7) along the total quartz-lithic leg in the "recycled orogen area" in the conventional triangular compositional diagram (Dickinson and Suczek 1979). The presence of well-sorted round quartz and relatively abundant metamorphic lithics may indicate derivation from the initial unroofing of an uplifted quartz-rich and metamorphic lithic-rich Gondwana continental assemblage during the final break-up event of Gondwanaland in the Cretaceous.

The lithic wackes of the Tianba Flysch are characterized by poorly sorted subangular quartz with significantly more lithic content. Quartz is dominant (average percentage, 62%), and inclusions of feldspar, biotite, and zircon in quartz grains are common. Matrix is generally abundant (10%–30%). Feldspar comprises 1%–6% of the total grain population. On the basis of extinction angles, plagioclase compositions range from albite to andesine and K-feldspar consists of either microcline or perthite. Sedimentary rock fragments (siltstone, shales, micritic limestones) are generally present (2%–3%) in medium and coarser sandstones. Metamorphic grains (1%–4%) are also present in small amounts. Volcanic clasts (2%–5%) contained in the wackes are both mafic and silicic in composition, although the larger clasts tend to be mafic. The presence of clear trachytic textures in some lithic grains indicates that the lithic wackes were derived from a terrane that included volcanic rocks. The recalculated mean value of QtFL and QmFLt (fig. 7) of the lithic wackes also plots in the "recycled orogen" area. The presence of poorly sorted sub-

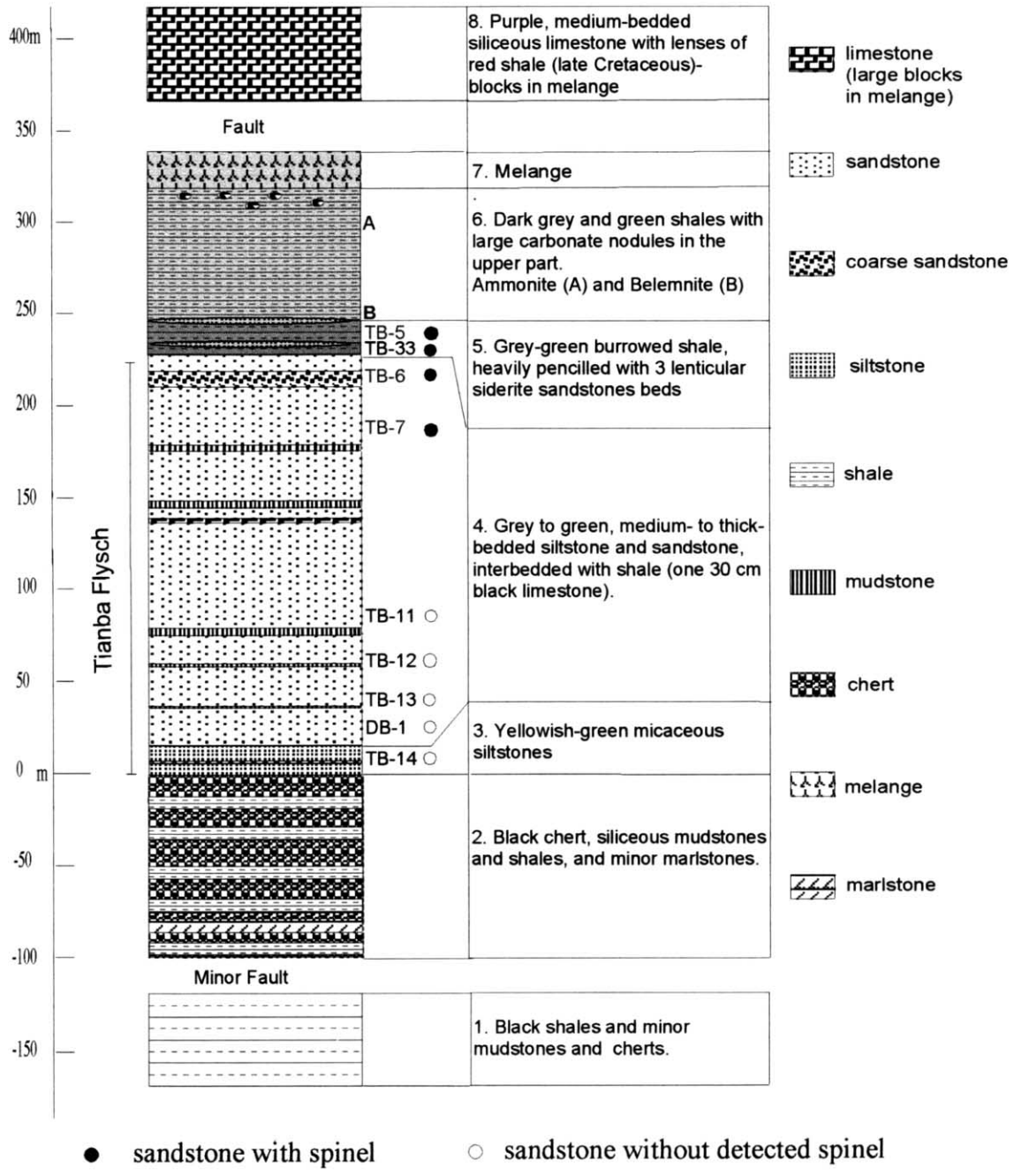

Figure 5. Detailed stratigraphic measured section (2) near Tianba, northern Nieru Valley

angular quartz suggests a short transport distance from the source rocks to the site of final deposition.

In summary, these arenites of the north Nieru Valley sections have similar quartz contents. However, lithic wackes have more matrix, feldspar, and volcanic lithic clasts and less metamorphic lithics. This change may indicate progressive unroofing of a crystalline basement with a partial sedimentary platform cover while at the same time having an increasingly significant volcanic component.

Heavy Mineral Analysis of Tianba Flysch

As stated earlier, many keynote works have demonstrated that heavy mineral analysis is a sensitive and well-proven technique for determining the

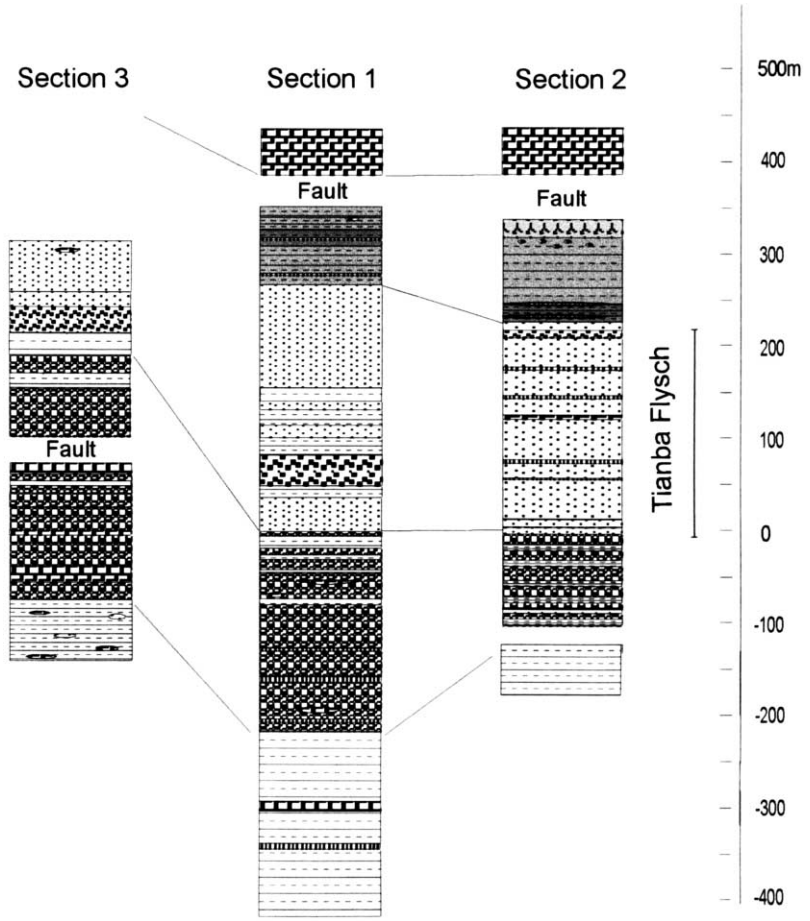

Figure 6. Measured stratigraphic sections in the northern Nieru Valley. Section locations are shown in figure 3. Symbols used for lithologies are the same as in figure 5.

provenance of clastic sediments (Morton 1991; Caironi et al. 1996; Lihou and Mange-Rajetzky 1996; Sciunnach and Garzanti 1996; Dewey and Mange 1999). Given the fact that some species derive from restricted lithologies, their detrital occurrence points to a clear source affinity (Dewey and Mange 1999). To date, no studies have reported quantitative and temporal variations in heavy-mineral assemblages from the Cretaceous sandstones in southern Tibet. Therefore, a study of heavy minerals in the Tianba Flysch was performed to better understand the tectonic history in southern Tibet during the Cretaceous.

Sample Preparation and Analytical Method

Nine samples were selected for heavy-mineral analysis (fig. 5). Samples were prepared using the standard laboratory technique (Mange and Maurer 1992) by separating out the heavy minerals from the 62.5–250-μm disaggregated fine-sand fraction using bromoform (tribromoethane, density 2.89). Analysis of the heavy-mineral population indicates a low-diversity, zircon-rich assemblage with varying amounts of tourmaline, apatite, rutile, magnetite, pyrite, and Cr-rich spinel. A significant volcanic component in the Tianba Flysch is reflected by the abundance of euhedral, colorless zircons in the upper part of the unit (TB6 and TB7). Cr-rich spinels were observed in four samples (TB6, TB7, TB5, and TB33). Since >50% of opaque minerals in the dense population of TB5 and TB33 are Cr-rich spinels, an ultramafic and/or mafic source terrane was important for these sediments. To the best of our knowledge, this is the first reported occurrence of Cr-rich spinels found in the mid–Late Cretaceous sandstones in southern Tibet. These detrital spinels are hence used to constrain the tectonic setting of the source area for the Tianba Flysch.

Eighty-one spinel grains were handpicked from

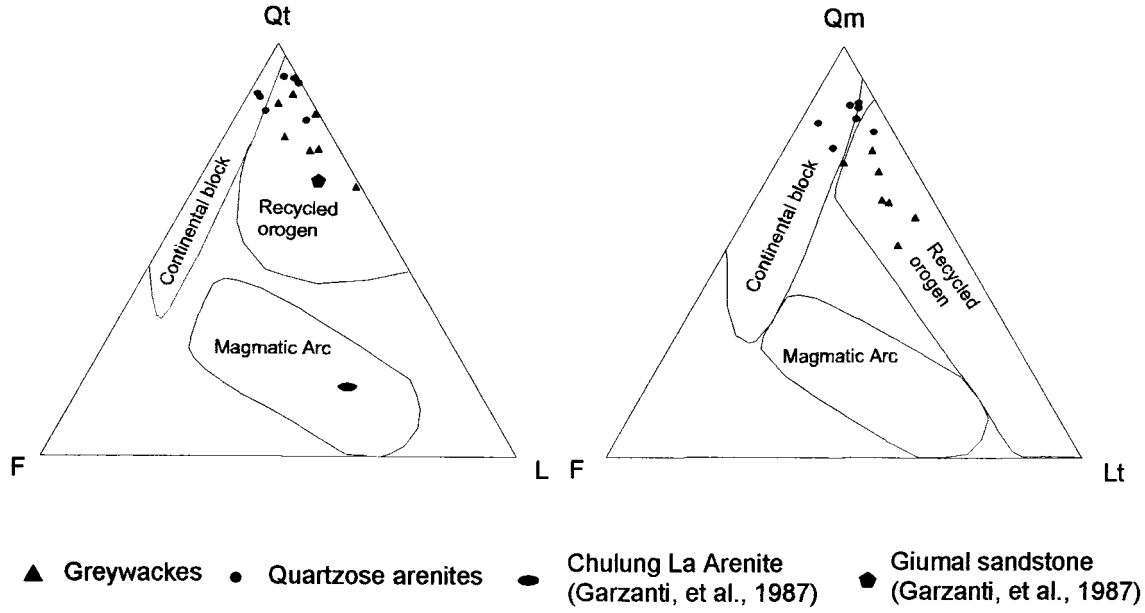

Figure 7. Detrital mode plot of Tianba Flysch. Tectonic fields are from Dickinson and Suczek (1979). Giumal sandstones and Chulung La Arenite from Zanskar (Garzanti et al. 1987) are shown for reference on the QtFL plot.

four samples (TB6, TB7, TB5, and TB33), individually mounted in epoxy resin, and ground and polished to expose the spinels for microprobe analysis. They are dark brown to dark reddish-brown and are up to 200 μ in diameter, with the majority being 100 μ. Some grain margins commonly show conchoidal fractures, suggesting mechanical breakage, whereas other grains are subhedral-euhedral and preserve the original crystal boundary. The occurrence of euhedral crystals suggests that original chemical zonation produced during crystallization from the parental magma may be preserved in those grains.

All analyses were performed using a JEOL 733 Superprobe (fully automated, five wavelength dispersive spectrometers) in the Department of Earth and Environmental Sciences at Rensselaer Polytechnic Institute. The elements Al, Mg, Cr, Fe, Ni, V, Mn, Zn, and Ti were analyzed under the following conditions: accelerating voltage 15 keV, beam current 15 na, and a beam diameter of 1 μ, ZAF correction model. The major elements were counted for 40 s and minor elements Ti, Mn, Ni, V, and Zn for 100 s each. Minimum detection limits (MDL) of minor elements are 0.0281% for Ni, 0.0635% for Zn, 0.0491% for Ti, and 0.0278% for Mn. USNM 117075 from Tiebaghi Mine, New Caledonia, was used as standard for Cr, Al, Fe, and Mg. Other element standards were as follows: Zn on pure gahnite; Ti on rutile; Mn on tephroite, V on synthetic V_2O_5, and Ni on diopside glass. Analysis of a spinel standard (USNM 117075) was done at the beginning, middle, and end of each analytical session to assess proper calibration. The analyses of this spinel standard for the six probe sessions showed no statistically significant differences. Each spinel grain was analyzed at two to six spots.

All Fe is expressed as FeO except for the first session, and the ferric iron content of each analysis was determined by assuming stoichiometry and an ideal XY_2O_4 formula (where X = Fe^{2+}, Mg, Ni, Zn; and Y = Cr, Al, Ti, Fe^{3+}), following the methods of Barnes and Roeder (2001). A recent study of Kamperman et al. (1996), using direct oxygen measurement of Cr-rich spinel, revealed that spinels from the volcanic rocks of Hunter Fracture Zone, Ca-rich boninites from the Tonga Trench, and metamorphosed volcanics from the Peak Hill–Glengarry Basin and the Heazlewood River Ultramafic Complex show a range of nonstoichiometry because of the cation deficiency in the spinel crystal structure. Barnes and Roeder (2001) also mentioned that the propagation of errors in the stoichiometry-based calculations might cause a significant error in the observed variance in trivalent ions. Given the fact that there are few analyses of direct oxygen measurement in spinels available and most concentrations of ferric and ferrous iron were calculated assuming ideal stoichiometry in the literature, we can only recognize this as a lim-

itation in the interpretation of the chemical composition of spinels (Barnes and Roeder 2001).

Cr-Rich Spinel Chemical Compositions

The microprobe results (table 1) indicate that the spinels from the Tianba Flysch contain 15%–26% Al_2O_3, 36%–45% Cr_2O_3, 10%–12% MgO, 20%–30% FeO_t, and 1.5%–2.0% TiO_2 (fig. 8). There is an obvious inverse relationship between Cr and Al, which may be indicative of different degrees of partial melting in the mantle (Dick and Bullen 1984). Mn, Ni, V, and Zn are typically present in only trace abundance, generally <0.5% oxides. No rim of "ferritchromit" was found in the spinels probed, and grains are generally homogeneous and show no obvious signs of zoning in line scans. This indicates that (1) parental lavas had undergone little or no magma mixing or significant crustal assimilation (Allan et al. 1988); (2) there was no extensive subsolidus reequilibration between spinels and other silicate minerals (Scowen et al. 1991); and (3) no major metamorphic event occurred after the crystallization of these spinels. Cr-spinels from the flysch (TB6 and TB7) appear to have a higher Mg/(Mg + Fe^{2+}) ratio and higher Al abundance then those from TB5 and TB33.

Volcanic Source for the Detrital Spinels

Most spinel-peridotites have spinels with low or negligible TiO_2 contents (except spinels in the plagioclase-peridotites from the Romanche Fracture Zone and St. Paul's Rocks [Dick and Bullen 1984]), whereas volcanic spinels with $TiO_2 < 0.2$ are uncommon (some suites of low-Ti MORB, arc tholeiites, and boninites [Kamenetsky et al. 2001]). Lenaz et al. (2000), therefore, set a compositional boundary between peridotitic and volcanic spinels at $TiO_2 = 0.2\%$. Given the fact that TiO_2 contents of our spinels are well above 0.2% (fig. 8), we conclude that the detrital spinels from Tianba Flysch were derived from volcanic rocks.

About 5% of the spinel grains contain melt inclusions and are thus of clear volcanic origin. Inclusions range in size from 10 to 40 μ. The phase assemblages observed among this suite of melt inclusions range from glass with some shrinkage bubbles (fig. 9*a*) to pyroxene blebs, residual glass, shrinkage vapor bubbles, and minor sulfide droplets (fig. 9*b*), and clinopyroxene. The presence of well-crystallized clinopyroxene (fig. 9*b*) indicates that there was a relatively long cooling history after entrapment. The compositions of four pyroxenes in this inclusion show that they have significantly different contents in the major oxides, as expected from closed-system crystallization; this is consistent with the interpretation that the pyroxenes are not xenocrystals but true daughter crystals formed after entrapment in the spinel. One spinifex-like texture was also found containing acicular clinopyroxene crystals (fig. 9*c*). The observed crystals at exposed surfaces of melt inclusions are randomly oriented relative to the crystallographic axes of host chromites, suggesting that there is similar arrangement in three dimensions. This distribution is similar to the olivine-enriched melt inclusions in chromites from low-Ca boninites, Cape Vogel, Papua New Guinea (Kamenetsky et al. 2002).

Minor Elements in the Detrital Spinels

Concentrations of MnO in the detrital spinels range from 0.17% to 0.43%, with a mean value of 0.25%. There is also a strong linear negative correlation between MnO and MgO (fig. 8). Since nearly all of our data (96%) plot (fig. 10*a*) below the boundary line (Barnes 1998) in the plot of MnO versus Mg number [Mg/(Mg + Fe^{2+})], we conclude that there were no significant chemical changes after crystallization of these spinels.

NiO abundances in the range of 0.076%–0.285% and positive correlations with MgO are observed (fig. 8). The content of Ni is inversely correlated with Cr/(Al + Cr + Fe^{3+}) and directly correlated with Mg number (fig. 10*b*) due to its large octahedral site preference in the chromian spinel structure (Paktunc and Cabri 1995). This is also consistent with the studies of Stosch (1981), who concluded that the composition of magma and coexisting olivine and spinel predominantly control Ni partitioning between Cr-rich spinels and mantle silicates.

ZnO abundance measured in 20 grains is consistently low (<0.20%). ZnO and Mg number are negatively correlated (fig. 10*c*), which may be indicative of Zn having a strong tetrahedral site preference in the crystal lattice of Cr-rich spinels (Paktunc and Cabri 1995). Of the 46 probed spinels, V_2O_5 abundances display a good correlation with Mg number as well (fig. 10*d*) and implies that V may also favor the tetrahedral site when entering the spinel structure.

In summary, Mn, Zn, and V are inversely correlated with Mg number, whereas Ni correlates positively with Mg number because of different site preferences. The correlations among these elements and Mg number suggest that they are sen-

Table 1. Representative Analyses of Cr-Rich Spinels from Tianba Flysch

Sample	TiO_2	V_2O_5	Al_2O_3	Cr_2O_3	MnO	MgO	NiO	ZnO	FeO	Fe_2O_3	Total	Cr/3+	Fe^{3+}/3+	Al/3+	Mg/(Mg + Fe^{2+})	Cr/(Cr + Al)
TB33	2.81	NA	17.10	39.09	.23	12.26	.18	.09	15.43	13.20	100.37	.49	.19	.32	.52	.61
TB33	1.64	NA	16.18	44.24	.26	10.93	.15	.09	16.74	11.52	101.76	.55	.15	.30	.48	.65
TB33	2.33	NA	17.58	37.95	.30	8.84	.15	.18	19.55	12.39	99.25	.49	.17	.34	.39	.59
TB33	2.34	NA	18.39	37.46	.30	9.06	.15	.17	19.47	12.18	99.52	.48	.17	.35	.40	.58
TB33	1.84	NA	19.69	37.94	.20	11.84	.14	BD	15.69	12.85	100.19	.46	.18	.36	.51	.56
TB33	3.36	NA	16.32	38.71	.43	12.29	.14	.13	14.74	10.86	96.98	.52	.16	.32	.54	.61
TB33	1.47	NA	16.45	42.11	.22	11.47	.13	.06	15.27	12.53	99.71	.52	.17	.30	.51	.63
TB5	2.34	.32	22.77	36.00	.33	20.78	.16	NA	5.09	12.27	100.06	.42	.19	.39	.82	.52
TB5	1.61	.36	16.36	40.71	.31	9.89	.13	NA	17.80	12.85	100.03	.51	.18	.31	.44	.63
TB5	1.46	.18	17.64	41.92	.25	11.70	.11	NA	15.67	12.14	101.06	.51	.16	.32	.51	.61
TB5	1.37	.18	18.91	42.52	.23	11.35	.15	NA	16.40	9.26	100.37	.53	.12	.35	.50	.60
TB5	1.40	.28	19.47	39.00	.25	11.42	.14	NA	16.21	12.73	100.90	.48	.17	.35	.49	.57
TB5	1.53	.17	20.09	37.77	.21	13.68	.16	NA	12.88	13.18	99.68	.46	.19	.36	.58	.56
TB5	1.95	.48	17.43	40.61	.37	10.02	.10	NA	18.33	10.48	99.78	.52	.14	.34	.44	.61
TB5	1.27	.28	19.18	40.53	.38	8.23	.11	NA	20.78	9.40	100.16	.52	.12	.36	.37	.59
TB5	4.24	.73	18.74	32.15	.30	7.97	.21	NA	23.23	11.66	99.24	.45	.17	.39	.34	.54
TB5	1.85	.29	18.28	37.89	.27	10.87	.14	NA	16.83	13.61	100.03	.47	.19	.34	.47	.58
TB5	1.96	.32	17.80	39.41	.21	13.08	.20	NA	13.77	12.91	99.66	.49	.18	.33	.56	.60
TB5	1.08	NA	23.03	39.24	.17	14.09	.19	BD	12.81	10.26	100.87	.46	.13	.40	.60	.53
TB5	1.83	NA	18.41	38.19	.24	11.21	.16	.06	16.29	14.21	100.59	.47	.20	.34	.48	.58
TB5	1.79	NA	16.08	41.28	.24	11.27	.14	.06	15.36	12.02	98.23	.53	.17	.31	.50	.63
TB5	1.59	.31	18.81	37.32	.33	8.11	.14	NA	20.47	12.06	99.13	.48	.16	.36	.36	.57
TB5	2.02	.45	16.64	39.75	.24	11.37	.20	NA	16.44	14.19	101.30	.49	.20	.31	.48	.62
TB5	2.06	.35	17.32	41.20	.26	12.48	.17	NA	14.87	11.46	100.17	.52	.16	.32	.54	.62
TB5	2.07	.40	18.20	38.00	.26	11.10	.17	NA	16.85	13.25	100.30	.48	.18	.34	.48	.58
TB7	1.01	NA	23.42	38.69	.17	13.90	.19	BD	12.91	10.02	100.35	.46	.13	.41	.60	.53
TB7	1.08	.17	19.97	43.25	.17	15.27	.19	NA	10.25	7.86	98.21	.53	.11	.36	.67	.59
TB6	1.17	.16	23.44	38.16	.19	15.04	.20	NA	11.16	9.27	98.79	.46	.12	.42	.65	.52
TB6	1.30	NA	23.63	37.95	.22	14.14	.17	BD	12.43	8.62	98.46	.46	.11	.43	.62	.52
TB6	.47	NA	39.34	26.82	.22	17.88	.02	BD	9.62	5.22	99.58	.29	.06	.65	.73	.31

Note. The ferric iron content of each analysis was determined by assuming stoichiometry, following the methods of Barnes and Roeder (2001). BD = below detection limits; NA = no analysis; 3+ = Cr + Al + Fe^{3+}.

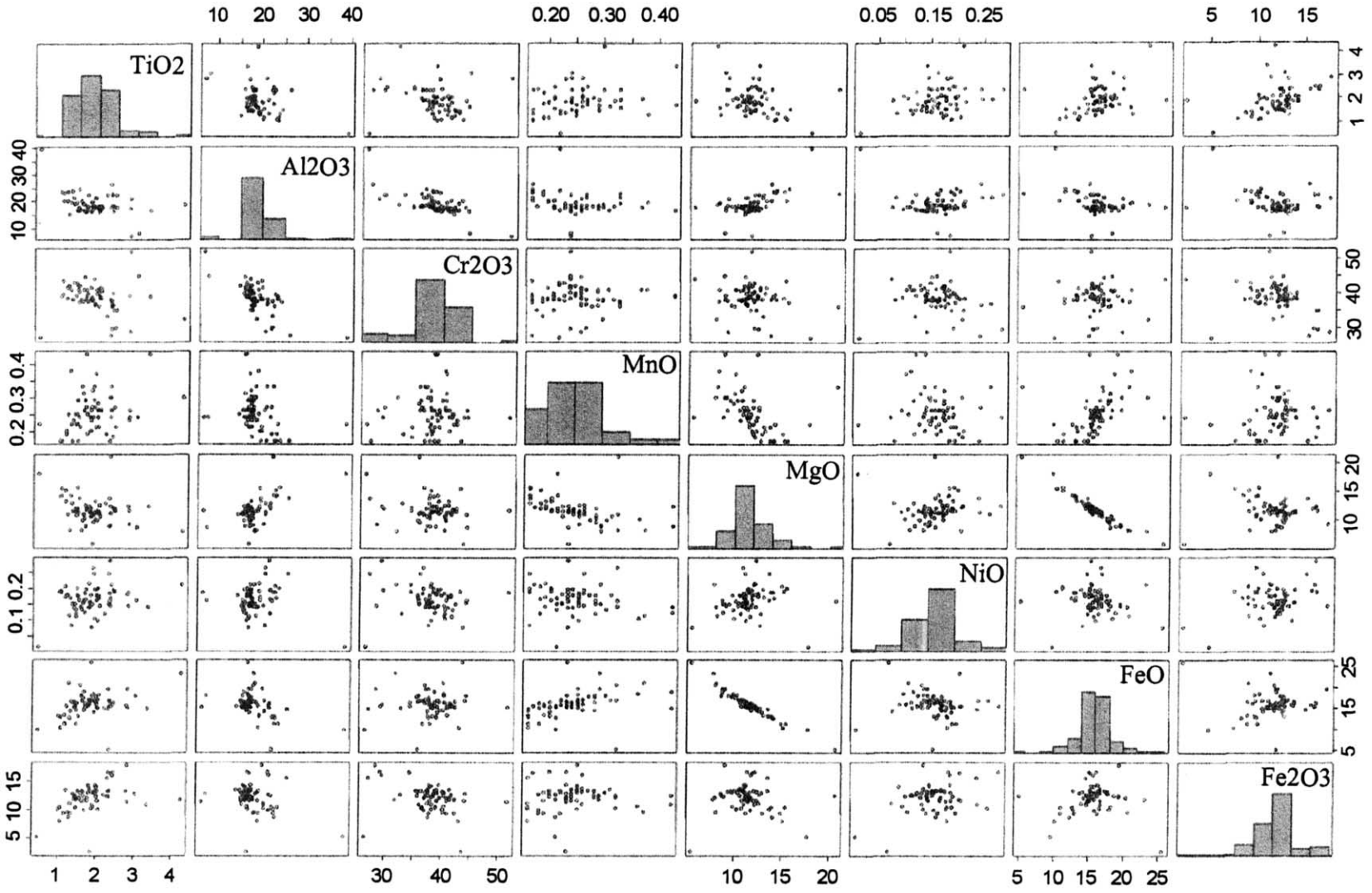

Figure 8. Chemical compositions of detrital Cr-rich spinels using pairs plot from S-Plus

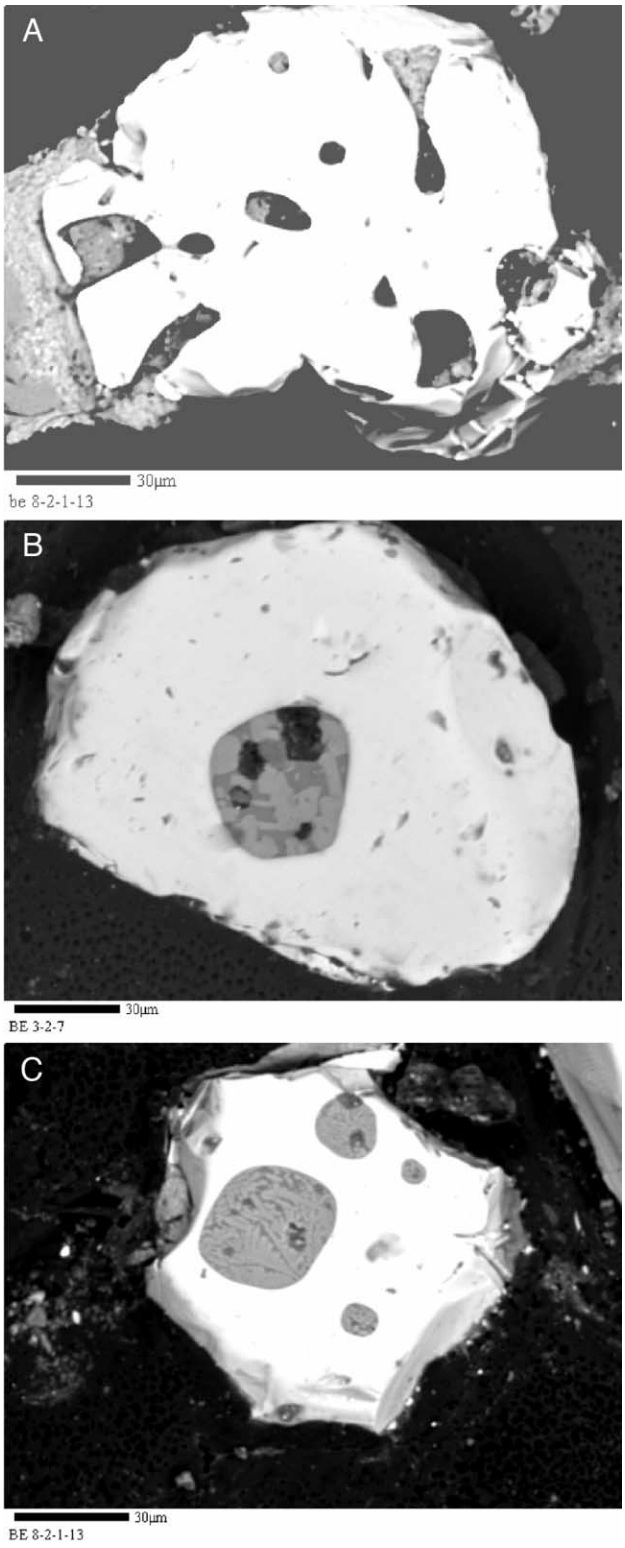

Figure 9. Backscattered electron images of melt inclusions in the detrital spinels from Tianba Flysch. Black bar below each image is 30 μm in length.

sitive to changes in the compositions of parental magma and coexisting early crystal phases. In addition, these results imply that there was a single source contributing the Cr-rich spinel to the Tianba Flysch.

Provenance of Cr-Rich Spinels

In the spinel nomenclature (Barnes and Roeder 2001), the detrital spinels we analyzed have a well-developed Fe-Ti trend and have Cr number $[Cr/(Cr + Al)] = 0.40$ to 0.65, Mg number $[Mg/(Mg + Fe^{2+})] = 0.3$ to 0.9, and $Fe^{3+}/(Al + Cr + Fe^{3+}) = 0.2$. In terms of the source terranes, it is well demonstrated that Cr-rich spinels from a variety of types of ultramafic and mafic complexes can be discriminated using specific combination of chemical parameters (e.g., Irvine 1967; Dick and Bullen 1984; Arai 1992; Barnes and Roeder 2001; Kamenetsky et al. 2001). Since overlaps among various tectonic settings on some plots (Dick and Bullen 1984) are not uncommon (Cookenboo et al. 1997), major, minor, and trace elements should be considered to determine the possible parental magmas of the spinels in the Tianba section.

In the plot of Cr number versus Mg number (fig. 11*a*), there is a slightly negative correlation between Cr number and Mg number, and the Mg number values are significantly scattered along the higher Cr number (close to 0.6). This may be a possible path of spinel crystallization due to the cocrystallization of olivine, plagioclase, and spinel (Roeder 1994) or a result of the prolonged crystallization of spinel and/or low-temperature reequilibration with olivine in host rocks (Lenaz et al. 2000; Kamenetsky et al. 2001). We favor the first interpretation because there is no evidence for significant low-temperature reequilibration observed as discussed previously. Comparison of our spinels with those coexisting with olivine in modern submarine volcanics (Kamenetsky et al. 2001) suggests that the studied spinels were most likely associated with primitive basalts with olivine phenocrysts at least as Mg-rich as Fo80-86 (fig. 11*a*). In the conventional fields (fig. 11*a*) of tectonic settings for spinels (Irvine 1967; Dick and Bullen 1984; Barnes and Roeder 2001), our data plot in the overlap field of oceanic island basalts (OIB) and MORB. As such, island arc tholeiites and boninites did not significantly contribute to these sedimentary strata.

Given the fact that the diffusivity of Ti, Al, and Cr through olivine is low (Scowen et al. 1991; Kamenetsky et al. 2001), and the contents of TiO_2 in the volcanic spinels increase from boninites and

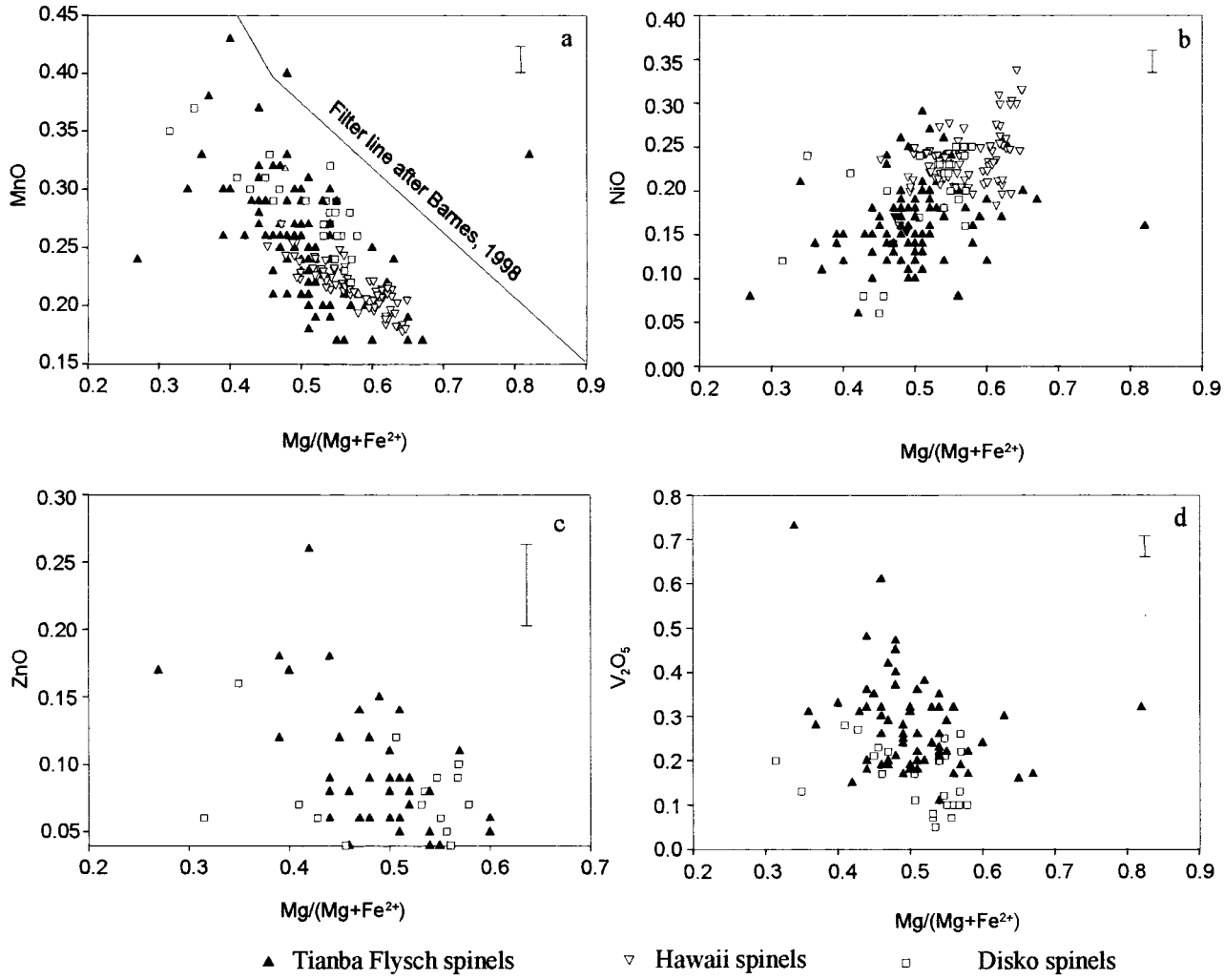

Figure 10. Covariation of minor elements with $Mg/(Mg + Fe^{2+})$ in spinel (for comparison, data from Hawaii and Disko are shown). *a*, MnO versus Mg number; *b*, NiO versus Mg number; *c*, ZnO versus Mg number; *d*, V_2O_5 versus Mg number. Vertical line on each plot represents the minimum detection limit for each minor element.

island arc basalts to intraplate basalts through MORB and back-arc basin basalts (Arai 1992), it is possible that these magma affinities can be distinguished by the relationship between Ti, Al, and Cr. In the plot of TiO_2 versus Cr number (fig. 11*b*), >90% of studied flysch spinels plot in the field of intraplate basalts with a few in the MORB field, but no points plot in island-arc basalt and boninite field. There is clear positive correlation between Ti and Fe^{3+} shown in the plot of TiO_2 versus $Fe^{3+}/(Al + Cr + Fe^{3+})$ (fig. 11*c*), which implies that there was a single source for these spinel in the Tianba Flysch (S. J. Barnes, pers. comm., 2003).

It appears that TiO_2 and Al_2O_3 are negatively correlative in Cr-rich spinels from hotspot and MORB, but not arc origins (fig. 11*d*), which may be indicative of reducing the partitioning of Ti into spinel with increasing Al activity in the system of melt-spinel because both favor the octahedral sites in the spinel structure (Kamenetsky et al. 2001). Using 400 melt inclusion-spinel pairs from 36 igneous suites from oceanic, arc, and intraplate tectonic environments, Kamenetsky et al. (2001) discriminated four fields of different geodynamic settings: continental flood basalt (CFB), oceanic island basalt (OIB), oceanic ridge basalt (MORB), and island-arc magmas (ARC) based on the relative contents of TiO_2 and Al_2O_3 in the studied spinels (fig. 11*d*). They also found that there is a strong positive correlation between TiO_2 and Al_2O_3 contents in spinel and coexisting melt inclusions, indicating that their contents in spinels are primarily dependent

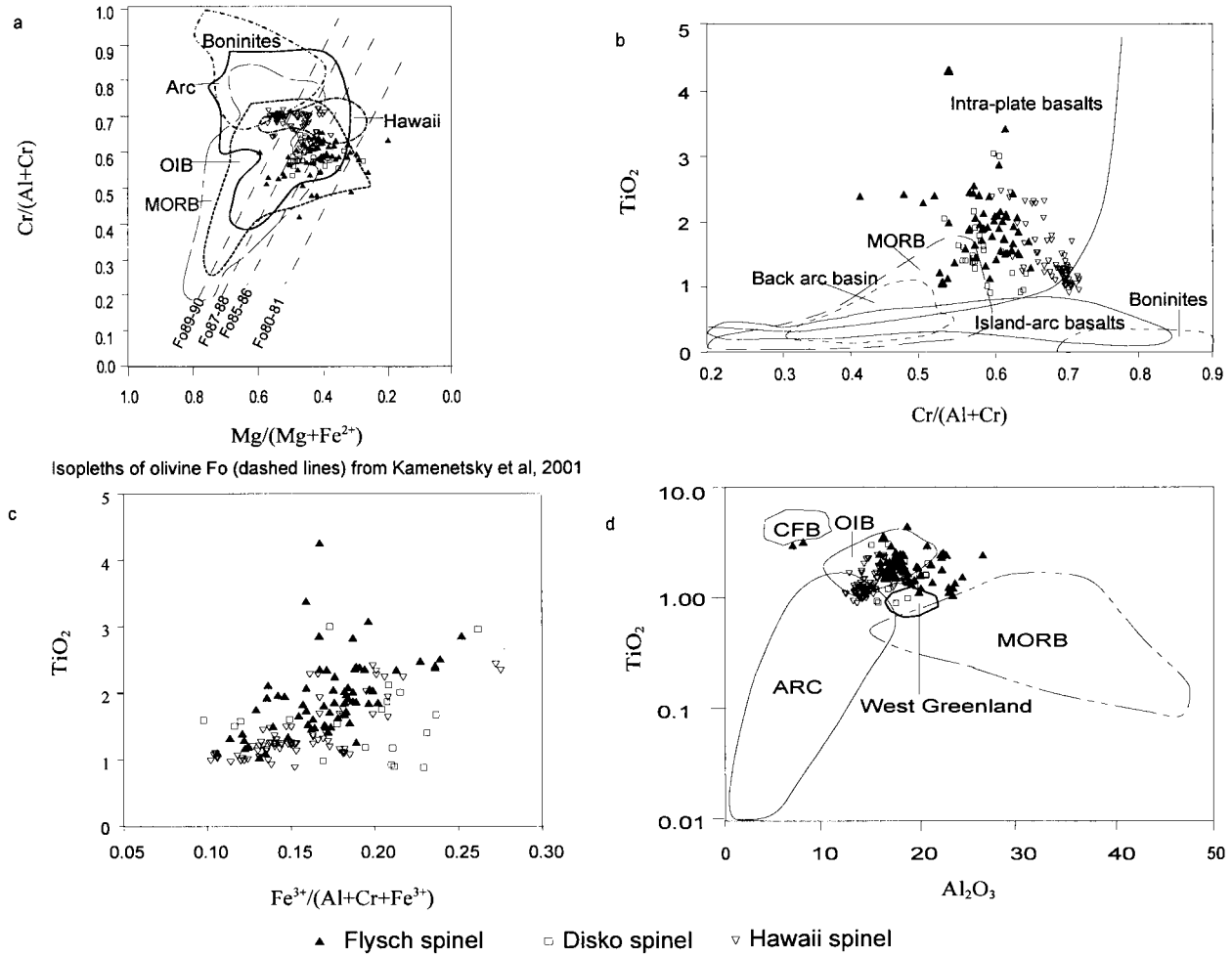

Figure 11. Major element contents of spinels and tectonic setting discriminant plot. *a*, $Cr/(Cr + Al)$ versus $Mg/(Mg + Fe^{2+})$ after Barnes and Roeder (2001); *b*, TiO_2 versus $Cr/(Cr + Al)$ after Arai (1992); *c*, TiO_2 versus $Fe^{3+}/(Al + Cr + Fe^{3+})$; *d*, TiO_2 versus Al_2O_3 after Kamenetsky et al. (2001).

on the magmatic TiO_2 and Al_2O_3 abundances, consistent with experimental studies of Roeder and Reynolds (1991). Plotting our flysch Cr-spinel data in their diagrams (not shown) for spinel-melt pairs (in terms of TiO_2 and Al_2O_3 abundances) indicates that the detrital spinels crystallized from a melt containing 13%–15% Al_2O_3 and 1.5–2.5 wt% TiO_2 (Zhu et al., unpub. manuscript), consistent with preliminary data of homogenized compositions of melt inclusions in the spinels. Most detrital spinels plot in the field of OIB (fig. 11*d*), which is consistent with the results of discriminant diagrams described previously.

Considered together, the binary plots of Mg number versus Cr number, TiO_2 versus Cr number, and TiO_2 versus Al_2O_3 demonstrate that the compositional range of the detrital spinels most closely matches that of spinels from OIBs and excludes island arc basalt, MORB, boninites, and ophiolites as significant sediment sources. Also shown (fig. 11) are spinels from Hawaii (spinel inclusions in olivine from Green Sand Beach; J. W. Delano, unpub. data) and from Late Cretaceous–Early Paleocene basalt of Disko Island, Greenland (Paktunc and Cabri 1995), both of hotspot affinity. It is clear that there are significant overlaps between spinels from Tianba Flysch, Hawaii, and Disko Island in these plots. Similar abundances (fig. 10) and similar trends in trace elements between spinels of the Tianba Flysch, Hawaii, and Disko Island, discussed previously, are also good indicators of close affinities of parental magma between these suites. Therefore, we conclude that our detrital spinels were derived from plume-related, hotspot basalts.

Discussion

Correlation of Tianba Flysch with the Giumal Group Sandstones in Zanskar. Lithic-rich arenites of the Cretaceous are widely exposed in the Tethyan Himalaya from Zanskar in the west to southeastern Tibet (Garzanti 1993; Durr and Gibling 1994). Comparisons of our stratigraphic data and sandstone detrital mode (fig. 7) with the well-documented Cretaceous sedimentary sequence in the northwest Himalaya show that the Giumal Group sandstones of the Zanskar region (Garzanti 1993) are analogous to the Tianba Flysch in many aspects (fig. 12). In Zanskar, the upper Jurassic to lower Cretaceous Spiti Shale is dominated by ammonite-bearing soft black calcareous shales and is conformably overlain by the Giumal Group. The latter has been subdivided into two formations (Garzanti 1993). The upper Necomian to Aptian Takh Formation is characterized by quartzo-feldspathic sandstones, whereas the Albian Pingdo La Formation consists of volcanic arenites and is capped by the Nerak and Oma Chu glauco-phosphorites. In the plot of QtFL (fig. 7), the Giumal sandstones plot in the "recycled orogen" field, similar to those of Tianba Flysch. The Giumal Group is immediately overlain by mudstones and shales with pelagic foraminifera (Chikkim Formation), beginning in the Late Albian or Early Turonian and reaching up to the Campanian/Maastrichtian boundary. The Cretaceous succession is completed by Maastrichtian marls and limestones (Kangi La and Marpo Formation).

Abundant fossils including ammonites (*Spiticeras, Neocosmoceras, Neocomites, Killanella*) and bivalves (*Inoceramus everesti, Oxytoma*) are reported in the upper part of the Spiti Shale (Wen 1987; Sinha 1988), indicating a Berriasian-Valangian age of deposition. There are also similar faunal assemblages in the lower part of the calcareous shales of the Jiabula Group in the eastern Himalaya. Therefore, available fossil evidence indicates that Cretaceous sedimentary rocks in the north Nieru Valley and Zanskar are correlative.

Continent-Wide, Early–Mid Cretaceous Volcanic Event. Clastic sediments correlative with the

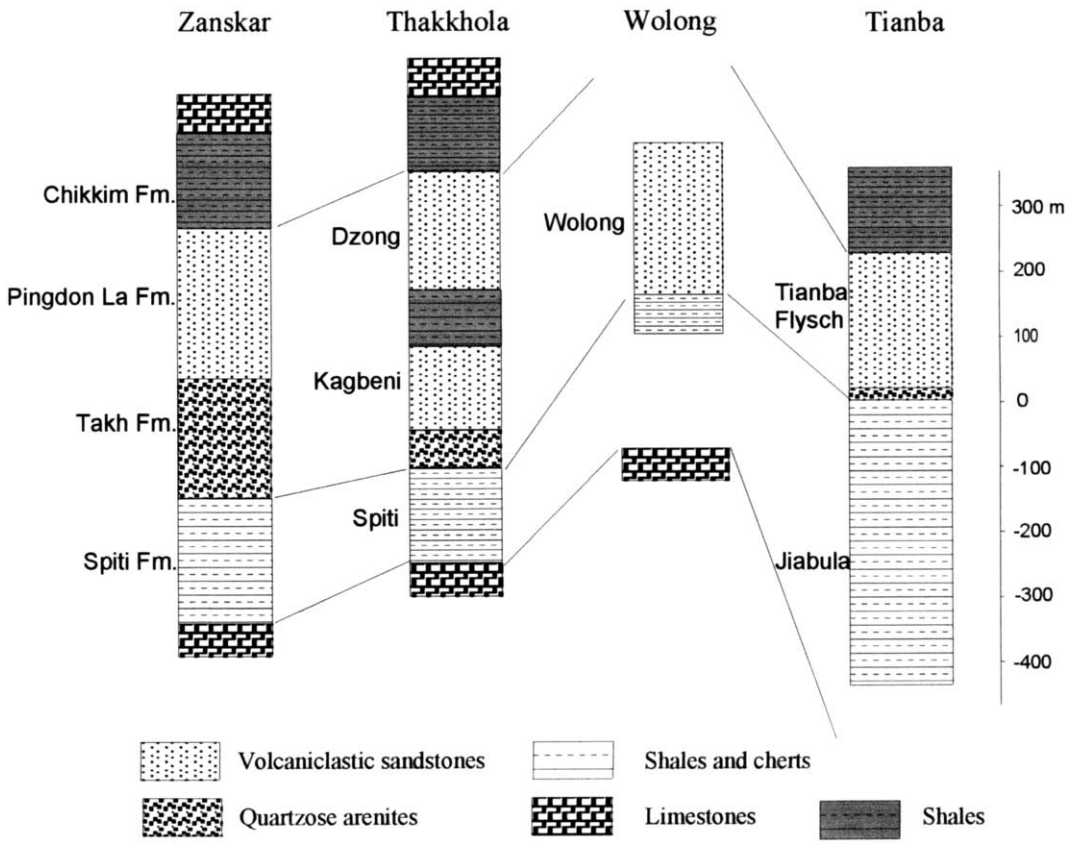

Figure 12. Comparison of lithostratigraphy between Tianba, Zanskar (after Garzanti 1993), Thakkhola (Garzanti 1999), and Wolong (Jadoul et al. 1998).

Tianba Flysch and Giumal Group are deposited throughout the Himalaya (fig. 12) from the Trans-Indus Salt Range, where siliciclastic deposits of Lumshiwal Formation accumulated in the Early Cretaceous (Hallam and Maynard 1987), to the Malla Johar and Thakkhola regions, where two >400-m-thick lithic wacke sections conformably overlie the ammonoid-rich black mudrocks of the Spiti Formation (Sinha 1988; Gibling et al. 1994), to southern Tibet, where early Cretaceous volcaniclastic sandstones are well exposed in the Wolong section (Jadoul et al. 1998). The geochemical composition of a basaltic pebble fragment found in the Valanginian to Aptian volcaniclastic sandstones in the Thakkhola region indicates a source of alkali basalts of within-plate affinity (Durr and Gibling 1994). The compositions of melt inclusions in the detrital spinels also point to a close affinity of alkali basalts (B. Zhu, J. W. Delano, W. S. F. Kidd, unpub. data). All basins of the East India coast are characterized by Early Cretaceous sandstones, which may reflect a rejuvenation of the craton due to lithospheric doming (Garzanti 1993). An upsurge of the Kerguelen mantle plume took place at 117 Ma (Kent 1991; Kent et al. 1997; Baksi 1995), erupting abundant flood basalt, as recorded in the Rajmahal-Sylhet-Bengal Trap Province of northeast India. Early Cretaceous volcaniclastic sediments are also found in the offshore sections of southeast Africa (Garzanti 1993). Therefore, tectonic extension affected both the western and eastern margins of the Indian continent in the Early Cretaceous.

The rapid increase in sand-sized quartzose detritus at the base in the Tianba Flysch indicates a significant exhumation of the source area when the Indian continent broke apart from the still-continuous East Gondwanaland supercontinent in the Early–mid Cretaceous (fig. 13). Relatively abundant volcanic detritus in the lithic wackes point to a large magmatic event. This temporal evolution is consistent with the classic sequence of tectono-sedimentary episodes during plume-related rifting. Initial doming is followed by erosion, tectonic extension, and rifting of a continent with reduction in the thickness of the lithosphere, followed by volcanic eruption at the climax above uprising hot plumes producing basaltic magma by extensive decompression melting of the asthenosphere (Campbell and Griffiths 1990; Garzanti 1993).

Late Jurassic to Cretaceous Oceanic Island Arc and Ophiolite Obduction. The presence of chrome-rich spinels in sedimentary rocks of a basin in and adjacent to an orogenic belt is generally interpreted as an indicator of derivation from an ophiolitic source (Pober and Faupl 1988; Cookenboo et al. 1997; Ganssloser 1999). As such, the presence of significant mafic volcanic detritus and uncharacterized chrome-rich spinels in the Tianba Flysch might suggest ophiolite derivation and a Cretaceous ophiolite obduction event on the northern Indian continental margin.

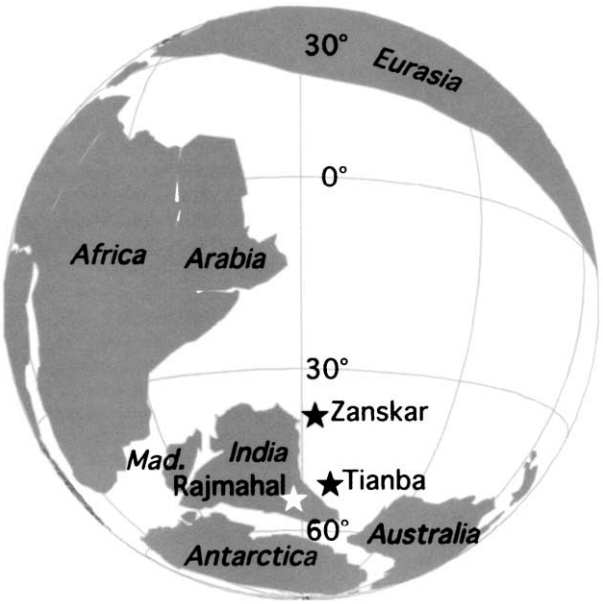

Figure 13. Paleogeography of the Tethys and surrounding continents at 117 Ma, showing the position of the Rajmahal volcanics, and the depositional sites of the mid-Cretaceous clastic sections now exposed in Zanskar and Tianba. A northward-directed subduction zone was probably located near or at the Eurasian margin. Base map from the Paleogeographic Atlas Project, University of Chicago.

It has been proposed (Searle 1983) that there was a Late Cretaceous ophiolite-obduction event recorded in the Zanskar region, northwestern Himalaya. Aitchison et al. (2000), McDermid et al. (2002), and Davis et al. (2002) show that there was a Late Jurassic to Early–mid Cretaceous intra-oceanic magmatic arc between the Indian passive margin and Lhasa block in southeastern Tibet. The Zedong terrane comprises basaltic-andesites, andesites, andesitic breccias, rare dacites, and other intrusives, as well as radiolarian cherts. South of it lies the Dazhuqu terrane, which consists of chert, siliceous mudstone, felsic tuffs, and fine-grained volcaniclastic turbidites, and the Bainang terrane, which is a series of south-directed imbricate thrusts including slices of red ribbon-bedded cherts, fine-grained siliciclastics, and tuffaceous cherts of Tethyan origin (Aitchison et al. 2000; McDermid et

al. 2002). This triad has been interpreted as representing the arc massif, the fore-arc basin, and the subduction complex of a deformed arc-trench system of Late Jurassic to Early–mid Cretaceous age within the Neo-Tethys (Aitchison et al. 2000; McDermid et al. 2002).

It is generally accepted that a Cr number >0.7 in spinel is indicative of arc-related setting (Dick and Bullen 1984), in contrast to the generally lower values of this ratio in spinel from MORB and OIB. Given the fact that abyssal ocean crust may be finally transported to a subduction zone and "so become tectonically intermingled with arc ophiolites" (Stowe 1994, p. 537), a wide variation in the chemical compositions would be expected for the spinels derived from arc complexes and associated accretionary complexes. TiO_2 content in arc spinels is generally <1 wt% (fig. 11). As described previously, there is, however, a narrow range of parameters for chemical compositions of the Tianba Flysch detrital spinels; most of them have TiO_2 abundance of ~2 wt%, and consistently plot in the discriminant field of OIB or intraplate basalts. No significant contribution to the Tianba Flysch has been detected of spinels with compositions matching those arc-trench complexes.

The close proximity of our sampled section to the Zedong-Dazhuqu-Banang region (fig. 1) requires that these arc-related accretionary materials did not affect this area until after deposition of the Tianba Flysch. As such, the northeastern Indian passive margin was not involved in tectonic interactions with Neo-Tethyan oceanic arc terranes during the mid-Cretaceous period when the Tianba Flysch was deposited.

Conclusions

Chrome-rich spinels occur in turbiditic sandstones from the upper part of mid-Cretaceous Tianba Flysch in the northern Nieru Valley, southern Tibet. Based on the presence of melt inclusions and >1% TiO_2 in the probed spinels, we conclude that the spinels were derived from a volcanic source. From the chemical compositions of the Cr-rich spinels, likely source rocks for these spinels are not arc-complexes or plutons or ophiolites, but flood basalts associated spatially and temporally with Kerguelen hotspot activity at 117 Ma, related to the break up of India, Australia, and Antarctica in the Early–mid Cretaceous. Although the Tianba Flysch looks in the field like a typical collisional product, and the presence of Cr-rich spinels might suggest an ophiolitic source and a Cretaceous ophiolite obduction event on the northeastern Indian continental margin, our detailed work shows clearly that the Tianba Flysch is neither ophiolite derived nor related to the start of the India-Asia collision.

ACKNOWLEDGMENTS

We thank J. Delano for extensive discussions and help in microprobe analysis of glasses in spinels and experimental procedures for heavy mineral separation, as well as for the use of his laboratory for this study. Discussions with G. Harper, J. Arnason, E. Garzanti, A. Baksi, V. Kamenetsky, I. Sigurdsson, and P. Roeder also have been of great help during this work. Microprobe work was assisted by K. Becker. Special thanks go to Binggao Zhang for helping in the field. We appreciate the detailed reviews of S. Barnes and an anonymous reviewer, which greatly improved the manuscript. This work was funded by a National Science Foundation Tectonics Program Grant to W. S. F. Kidd and D. B. Rowley and a State University of New York Albany Benevolent Fund Research Grant to B. Zhu.

REFERENCES CITED

Aitchison, J.; Badengzhu; Davis, A.; Liu, J.; Luo, H.; Malpas, J.; McDermid, I.; Wu, H.; Ziabrev, S.; and Zhou, M. 2000. Remnants of a Cretaceous intra-oceanic subduction system within the Yarlung-Zangbo suture (southern Tibet). Earth Planet. Sci. Lett. 183:231–244.

Allan, J. F.; Sack, R. O.; and Batiza, R. 1988. Cr-rich spinels as petrogenetic indicators: MORB-type lavas from the Lamont seamount chain, eastern Pacific. Am. Mineral. 73:741–753.

Allegre, C.; Courtillot, V.; Tapponnier, P.; Hirn, A.; Mattauer, M.; Coulon, C.; Jaeger, J. J.; et al. 1984. Structure and evolution of the Himalayas-Tibet orogenic belt. Nature 307:17–22.

Arai, S. 1992. Chemistry of chromian spinel in volcanic rocks as a potential guide to magma chemistry. Mineral. Mag. 56:173–184.

Arai, S., and Okada, H. 1991. Petrology of serpentine sandstone as a key to tectonic development of serpentine belts. Tectonophysics 195:65–81.

Baksi, A. K. 1995. Petrogenesis and timing of volcanism in the Rajmahal flood basalt province, NE India. Chem. Geol. 121:73–90.

Barnes, S. J. 1998. Chromite in komatiites. I. Magmatic control on crystallization and composition. J. Petrol. 39:1689–1720.

Barnes, S. J., and Roeder, P. L. 2001. The range of spinel compositions in terrestrial mafic and ultramafic rocks. J. Petrol. 42:2279–2302.

Beck, R. A.; Burbank, D. W.; Sercombe, W. J.; Riley, G. W.; Barndt, J. K.; Berry, J. R.; Afzal, J.; et al. 1995. Stratigraphic evidence for an early collision between northwest India and Asia. Nature 373:55–58.

Burg, J., and Chen, G. 1984. Tectonics and structural formation of southern Tibet, China. Nature 311:219–223.

Caironi, V.; Garzanti, E.; and Sciunnach, D. 1996. Typology of detrital zircon as a key to unraveling provenance in rift siliciclastic sequences (Permo-Carboniferous of Spiti, N India). Geodinamica Acta 9:101–113.

Campbell, I. H., and Griffiths, R. W. 1990. Implications of mantle plume structure for the evolution of flood basalts. Earth Planet. Sci. Lett. 99:79–93.

Cookenboo, H. O.; Bustin, R. M.; and Wilks, K. R. 1997. Detrital chromian spinel compositions used to reconstruct the tectonic setting of provenance: implications for orogeny in the Canadian Cordillera. J. Sediment. Res. 67:116–123.

Davis, A.; Aitchison, J.; Badengzhu; Luo, H.; and Zyabrev, S. 2002. Paleogene island arc collision-related conglomerates, Yarlung-Tsangpo suture zone, Tibet. Sediment. Geol. 150:247–273.

Dewey, J., and Mange, M. 1999. Petrography of Ordovician and Silurian sediments in the western Irish Caledonides: tracers of short-lived Ordovician continent-arc collision orogeny and the evolution of the Laurentian Appalachian-Caledonian margin. *In* Mac Niocaill, C., and Ryan, P. D., eds. Continental tectonics. Geol. Soc. Lond. Spec. Pub. 164:55–107.

Dick, H. J. B., and Bullen, T. 1984. Chromian spinel as a petrogenetic indicator in abyssal and alpine-type peridotites and spatially associated lavas. Contrib. Mineral. Petrol. 86:54–76.

Dickinson, W. 1985. Interpreting provenance relations from detrital modes of sandstones. *In* Zuffa, G, ed. Provenance of arenites. Dordrecht, Netherlands, Reidel, NATO Advanced Study Inst. Series 148:333–361.

Dickinson, W., and Suczek, C. 1979. Plate tectonics and sandstones composition. Geol. Soc. Am. Bull. 63: 2164–2172.

Durr, S. 1996. Provenance of Xigaze fore-arc basin clastic rocks (Cretaceous, South Tibet). Geol. Soc. Am. Bull. 108:669–684.

Durr, S., and Gibling, M. R. 1994. Early Cretaceous volcaniclastic and quartzose sandstones from north central Nepal: composition, sedimentology and geotectonic significance. Geol. Rundsch. 83:62–75.

Einsele, G.; Liu, B.; Durr, S.; Frisch, W.; Liu, G.; Luterbacher, H. P.; Ratschbacher, L.; et al. 1994. The Xigaze forearc basin, evolution and facies architecture (Cretaceous, Tibet). Sediment. Geol. 90:1–20.

Gansslosser, M. 1999 Detrital chromian spinels in Rhenohercynian greywackes and sandstones (Givetain-Visean, Variscides, Germany) as indicators of ultramafic source rocks. Geol. Mag. 136:437–451.

Garzanti, E. 1993. Sedimentary evolution and drowning of a passive margin shelf (Giumal Group; Zanskar Tethys Himalaya, India): palaeoenvironmental changes during final break-up of Gondwanaland. *In* Treloar, P., and Searle, M., eds. Himalayan tectonics. Geol. Soc. Lond. Spec. Pub. 74:277–298.

———. 1999. Stratigraphy and sedimentary history of the Nepal Tethys Himalayan passive margin. J. Asian Earth Sci.17:805–827.

Garzanti, E.; Baud, A.; and Mascle, G. 1987. Sedimentary record of the northward flight of India and its collision with Eurasia (Ladakh Himalayas, India). Geodinamica Acta 1:297–312.

Garzanti, E.; Critelli, S.; and Ingersoll, R. 1996. Paleogeographic and paleotectonic evolution of the Himalayan Range as reflected by detrital modes of Tertiary sandstones and modern sands (Indus transect, India and Pakistan). Geol. Soc. Am. Bull. 108:631–642.

Gibling, M. R.; Gradstein, F. M.; Kristiansen, I. L.; Nagy, J.; Sarti, M.; and Wiedmann, J. 1994. Early Cretaceous strata of the Nepal Himalayas: conjugate margins and rift volcanism during Gondwanan breakup. J. Geol. Soc. Lond. 151:269–290

Hallam, A., and Maynard, J. B. 1987. The iron ores and associated sediments of the Chichali formation (Oxfordian to Valanginian) of the Trans-Indus Salt Range, Pakistan. J. Geol. Soc. Lond. 144:107–114.

Ingersoll, R. V.; Bullard, T. F.; Ford, R. L.; Grimm, J. P.; Pickle, J. D.; and Sares, S. W. 1984. The effect of grain size on detrital modes: a test of the Gazz-Dickinsion point-counting method. J. Sediment. Petrol. 49:103–116.

Irvine, T. N. 1967. Chromium spinel as a petrogenetic indicator. II. Petrologic applications. Can. J. Earth Sci. 4:71–103.

Jadoul, F.; Berra, F.; and Garzanti, E. 1998. The Tethys Himalayan passive margin from Late Triassic to Early Cretaceous (South Tibet). J. Asian Earth Sci. 16:173–194.

Kamenetsky, V.; Crawforad, A. J.; and Meffre, S. 2001. Factors controlling chemistry of magmatic spinel: an empirical study of associated olivine, Cr-spinel and melt inclusions from primitive rocks. J. Petrol. 41: 655–671.

Kamenetsky, V.; Sobolev, A. V.; Eggins, S. M.; Crawford, A. J.; and Arculus, R. J. 2002. Olivine-enriched melt inclusions in chromites from low-Ca boninites, Cape Vogel, Papua New Guinea: evidence from ultramafic primary magma, refractory mantle source and enriched components. Chem. Geol. 183:287–303.

Kamperman, M.; Danyushevsky, L. V.; Taylor, W. R.; and Jablonski, W. 1996. Direct oxygen measurement of Cr-rich spinel: implication for spinel stoichiometry. Am. Mineral. 81:1186–1194.

Kent, R. 1991. Lithospheric uplift in eastern Gondwana: evidence for a long-lived mantle plume system? Geology 19:19–23.

Kent, R.; Saunders, A. D.; Kempton, P. D.; and Ghose, N. C. 1997. Rajmahal basalts, Eastern India: mantle sources and melt distribution at a volcanic rifted margin. *In* Mahoney, J. J., and Coffin, M. F., eds. Large igneous provinces: continental, oceanic, and planetary

flood volcanism. Washington, D.C., American Geophysical Union Monogr. 100, p. 145–182.
Lee, Y. 1999. Geotectonic significance of detrital chromian spinel: a review. Geosci. J. 3:23–29.
Lenaz, D.; Kamenetsky, V.; Crawford, A. J.; and Princivalle, F. 2000. Melt inclusions in detrital spinel from SE Alps (Italy-Slovenial): a new approach to provenance studies of sedimentary basins. Contrib. Mineral. Petrol. 139:748–758.
Lihou, J. C., and Mange-Rajetzky, M. A. 1996. Provenance of the Sardona Flysch, eastern Swiss Alps: examples of high-resolution heavy mineral analysis applied to an ultrastable assemblage. Sediment. Geol. 105:141–157.
Liu, G. 1992. Permian to Eocene sediments and Indian passive margin evolution in the Tibetan Himalaya. Tubinger Geowiss. Arb. 13:1–268.
Mange, M. A., and Maurer, H. F. W. 1992. Heavy mineral in color. London, Chapman & Hall, 147 p.
McDermid, I. R. C.; Aitchison, J. C.; Davis, A. M.; Harrison, T. M.; and Grove, M. 2002. The Zedong terrane: a Late Jurassic intra-oceanic magmatic arc within the Yarlung-Tsangpo suture zone, southeastern Tibet. Chem. Geol. 187:267–277.
Morton, A. C. 1985. Heavy minerals in provenance studies. *In* Zuffa, G. G., ed. Provenance of arenites. Dordrecht, Netherlands, Reidel, p. 249–277.
———. 1991. Geochemical studies of detrital heavy minerals and their application to provenance studies. *In* Morton, A. C.; Todd, S. P.; and Haughton, P. D. W., eds. Developments in sedimentary provenance studies. Geol. Soc. Lond. Spec. Pub. 57:31–45.
Paktunc, A. D., and Cabri, L. J. 1995. A proton- and electron-microprobe study of gallium, nickel and zinc distribution in chromian spinel. Lithos 35:261–282.
Pober, E., and Faupl, P. 1988. The chemistry of detrital spinels and its application for the geodynamic evolution of the Eastern Alps. Geol. Rundsch. 77:641–670.
Roeder, P. L. 1994. Chromite: from the fiery rain of chondrules to the Kilauea Iki lava lake. Can. Mineral. 32: 729–746.
Roeder, P. L., and Reynolds, I. 1991. Crystallization of chromite and chromium solubility in basaltic melts. J. Petrol. 32:909–934.
Rowley, D. 1996. Age of initiation of collision between India and Asia: a review of stratigraphic data. Earth Planet. Sci. Lett. 145:1–13.
———. 1998. Minimum age of initiation of collision between India and Asia north of Everest based on the subsidence history of the Zhepure Mountain section. J. Geol. 106:229–235.
Rowley, D., and Kidd, W. S. F. 1981. Stratigraphic relationships and detrital composition of the medial Ordovician flysch of western New England: implications for the tectonic evolution of the Taconic Orogeny. J. Geol. 89:199–218.
Sciunnach, D., and Garzanti, E. 1996. Detrital chromian spinels record tectono-magmatic evolution from Carboniferous rifting to Permian spreading in Neotethys (India, Nepal and Tibet). Ofioliti 22:101–110.
Scowen, P. A. H.; Roeder, P. L.; and Helz, R. T. 1991. Reequilibration of chromite within Kilauea Iki lava lake, Hawaii. Contrib. Mineral. Petrol. 107:8–20.
Searle, M. P. 1983. Stratigraphy, structure, and evolution of the Tibetan-Tethys zone in Zanskar and the Indus suture zone in Ladakh Himalaya. R. Soc. Edinb. Earth Sci. 73:205–219.
Sengor, A. M. C.; Altiner, D.; Cin, A.; Ustomer, T.; and Hsu, K. J. 1988. Original assembly of the Tethyside orogenic collage at the expense of Gondwanaland. *In* Audley-Charles, M. G., and Hallame, A., eds. Gondwana and Tethys. Geol. Soc. Spec. Pub. 37:119–181.
Sinha, A. 1988. Geology of the higher Central Himalaya. New York, Wiley, 219 p.
Stosch, H. G. 1981. Sc, Cr, Co and Ni partitioning between minerals from spinel peridotite xenoliths. Contrib. Mineral. Petrol. 78:166–174.
Stowe, C. W. 1994. Compositions and tectonic settings of chromite deposits through time. Econ. Geol. 89: 528–546.
Tapponnier, P.; Mercier, J. L.; Proust, F.; Andrieux, J.; Armijo, R.; Bassoullet, J. P.; Brunel, M.; et al. 1981. The Tibetan side of the India-Eurasia collision. Nature 294: 405–410.
Wan, X. Q.; Liang, D. Y.; and Li, G. B. 2001. Paleocene stratigraphic evidence for India-Asia collisional compression in Gamba, southern Tibet. J. Asian Earth Sci. 19:73–74.
Wang, C., et al. 2000. The Cretaceous in Gyangze, Southern Xizang (Tibet): redefined. Acta Geol. Sin. 74:97–107.
Wen, S. 1987. Cretaceous system. *In* Chinese Academy of Sciences, eds. Stratigraphy of the Mount Qomolangma Region. Beijing, Science, p. 130–159.
Willems, H.; Zhou, Z.; Zhang, B.; and Graefe, K. U. 1996. Stratigraphy of the upper Cretaceous and lower Tertiary strata in the Tethyan Himalayas of Tibet (Tingri area, China). Geol. Rundsch. 85:723–754.
Xizang BGMR (Xizang Bureau of Geology and Mineral Resources). 1992. Regional geology of the Xizang Autonomous Region. Beijing, Geological Publishing House.
Yin, A., and Harrison, M. 2000. Geologic evolution of the Himalayan-Tibetan orogen. Annu. Rev. Earth Planet. Sci. 28:211–280.
Ziabrev, S.; Aitchison, J.; Badengzhu; Davis, A. M.; and Luo, H. 2001. More about the Tethys in the Yarlung Zangbo suture. J. Asian Earth Sci. 19:82–83.
Zuffa, G. 1980. Optical analysis of arenites: their composition and classification. J. Sediment. Petrol. 50:21–29.